HHS Public Access

Author manuscript

J Tissue Eng Regen Med. Author manuscript; available in PMC 2015 March 20.

Published in final edited form as:

J Tissue Eng Regen Med. 2013 February ; 7(2): 99–111. doi:10.1002/term.497.

Effects of designed PLLA and 50:50PLGA scaffold architectures on bone formation *in vivo*

Eiji Saito[1], **Elly E. Liao**[1], **Wei-Wen Hu**[5], **Paul H. Krebsbach**[1,2], and **Scott J. Hollister**[1,3,4]

Scott J. Hollister: scottho@umich.edu

[1]Department of Biomedical Engineering, University of Michigan, Ann Arbor, Michigan 48109-2099

[2]Department of Biologic and Materials Science, School of Dentistry, University of Michigan, Ann Arbor, Michigan 48109-1078

[3]Department of Mechanical Engineering, University of Michigan, Ann Arbor, Michigan 48109-2125

[4]Department of Surgery, University of Michigan, Ann Arbor, Michigan 48109-0329

[5]Department of Chemical and Materials Engineering, National Central University, Jhongli, Taoyuan, Taiwan

Abstract

Biodegradable porous scaffolds have been investigated as an alternative approach to current metal, ceramic, and polymer bone graft substitutes for lost or damaged bone tissues. Although there have been many studies investigating the effects of scaffold architecture on bone formation, many of these scaffolds were fabricated using conventional methods, such as salt leaching and phase separation, and were constructed without designed architecture. To study the effects of both designed architecture and material on bone formation, we designed and fabricated three types of porous scaffold architecture from two biodegradable materials, poly (L-lactic acid) (PLLA) and 50:50Poly (lactic-co-glycolic acid) (PLGA) using image based design and indirect solid freeform fabrication techniques, seeded them with bone morphogenic protein-7 transduced human gingival fibroblasts and implanted them subcutaneously into mice for 4 and 8 weeks. Micro-computed tomography data confirmed that the fabricated porous scaffolds replicated the designed architectures. Histological analysis revealed that the 50:50PLGA scaffolds degraded and did not maintain their architecture after 4 weeks. The PLLA scaffolds maintained their architecture at both time points and showed improved bone ingrowth which followed the internal architecture of the scaffolds. Mechanical properties of both PLLA and 50:50PLGA scaffolds decreased, but PLLA scaffolds maintained greater mechanical properties than 50:50PLGA after implantation. The increase of mineralized tissue helped to support mechanical properties of bone tissue and scaffold constructs from 4 to 8 weeks. The results indicated the importance of choice of scaffold materials and computationally designed scaffolds to control tissue formation and mechanical properties for desired bone tissue regeneration.

1. Introduction

Bone graft substitutes such as titanium and other metals have been used for reconstructing bone defects caused by injury, inflammatory disease or cancer. However, these implants are

less than ideal because the materials are non-degradable and may cause stress shielding. Tissue engineered scaffolds have been studied as alternative implants to heal skeletal defects. To enhance bone tissue integration and bone growth into the tissue engineered scaffolds, the scaffolds should have porous architecture to encourage cell migration and blood vessel formation (Karageorgiou and Kaplan, 2005). It is also necessary to have sufficient mechanical properties to support physiologic loading, and proper degradation profiles to transfer loads to regenerating tissues during healing (Athanasiou *et al.*, 1998, Hutmacher, 2001, Hollister, 2005).

Poly (L-lactic acid) (PLLA) and Poly (lactic-*co*-glycolic acid) (PLGA) have both been approved by the FDA for specific clinical indications (Middleton and Tipton, 2000). They have been used as orthopaedic implants (Athanasiou *et al.*, 1998, Kontakis *et al.*, 2007) and have been widely studied as scaffolds for bone regeneration both *in vitro* and *in vivo*. Due to different degrees of hydrophilicity, degradation ratios and by-products, PLLA and PLGA have different effects on cell behavior and tissue regeneration, and have been compared in different matrices, including films, porous sponges, and fiber like shapes using various cell types (Narayan and Venkatraman, 2008, Li *et al.*, 2006, Kaushiva *et al.*, 2007, Ishaug-Riley *et al.*, 1999). It has been demonstrated that the degradation time changes depending on the ratio of lactic acid and glycolic acid polymer (Li *et al.*, 2006, Kaushiva *et al.*, 2007, Lu *et al.*, 2000). Thus, adjusting the polymer ratio should control the degradation time of these scaffolds and their distinct degradation profiles may influence bone regeneration.

In addition to the scaffold material composition, factors influencing scaffold architecture, such as porosity and pore size, play a critical role in cell migration and bone formation into the scaffolds (Gomes *et al.*, 2006, Khan *et al.*, 2008). It has been postulated that an approximately 100 μm pore diameter is suitable for *in vitro* cell migration and a 300 μm pore diameter is necessary for tissue ingrowth and nutrient diffusion (Karageorgiou and Kaplan, 2005, Cao *et al.*, 2006). However, the effects of scaffold architecture on bone tissue formation are not fully known, and vary significantly between studies (Schek *et al.*, 2006, Li *et al.*, 2007, Rose *et al.*, 2004, Tsuruga *et al.*, 1997, Kuboki *et al.*, 2001, Ishaug-Riley *et al.*, 1997, Ishaug-Riley *et al.*, 1998, Wu *et al.*, 2006). Because the effects of scaffold architecture on bone formation may differ depending on the materials studied (Wu *et al.*, 2006, Sinha *et al.*, 1994) and the ability to fabricate scaffolds with controlled pore architectures (Melchels *et al.*, 2010), it is necessary to investigate the effects of rigorously controlled architectures for each biodegradable scaffold to clearly delineate architecture versus material influence on bone regeneration.

Conventional biodegradable scaffolds, especially scaffolds made from PLLA and PLGA, have been commonly fabricated by salt leaching or gas foaming and have a wide range of pore sizes with poor or non-interconnected pores, and the scaffold architectures are not identically duplicated with repeated samples (Hsu *et al.*, 2007, Hutmacher *et al.*, 2001). It is also difficult to control local pore and wall locations, and porosities of these scaffolds. Currently, scaffold architecture is controlled in the global or overall scaffold level. Furthermore, in order to ensure pore interconnectivity, porosity needs to be increased, and as a result the mechanical properties of scaffolds may thus be reduced (Goldstein *et al.*, 1999).

To overcome these limitations, the combination of computer aided design and solid freeform fabrication techniques have been developed (Hollister, 2005, Sun *et al.*, 2004, Hutmacher *et al.*, 2004, Martins *et al.*, 2009). These methods allow design and fabrication of scaffolds with controllable local pore architecture to generate reproducible and effective mechanical and mass transport properties. Our group has developed image based design techniques by which the internal architectures of scaffolds can be customized based on the mathematical concept of unit cells (Hollister *et al.*, 2000, Hollister *et al.*, 2002, Lin *et al.*, 2004). These unit cells are designed and fabricated to have the desired effective physical properties, such as compressive modulus, permeability and diffusivity. Furthermore, we have utilized the indirect solid freeform fabrication (SFF) method to fabricate scaffolds with designed pore diameters, struts sizes and porosities (Taboas *et al.*, 2003). Utilizing these techniques, we have successfully designed and fabricated 50:50PLGA porous scaffolds which have compression moduli within the range of human trabecular bone (Saito *et al.*, 2010).

Bone morphogenetic proteins (BMPs) belong to the TGF-β family and had been extensively applied using direct BMP delivery or *in vivo* or *ex vivo* delivery via gene therapy to induce bone formation for skeletal regeneration (Bessa *et al.*, 2008a, Bessa *et al.*, 2008b, Nussenbaum and Krebsbach, 2006). Our method to express BMPs *in vivo* uses human dermal and gingival fibroblasts that have been transduced by recombinant adenovirus encoding BMPs to induce bone formation in ectopic sites (Rutherford *et al.*, 1992, Krebsbach *et al.*, 2000). This technique has also been combined with porous SFF scaffolds to facilitate bone generation (Schek *et al.*, 2006, Williams *et al.*, 2005, Lin *et al.*, 2005, Roosa *et al.*, 2010). Consequently, this *ex vivo* gene therapy method can be applied to induce bone formation in our engineered scaffolds.

The goal of this study was to determine the influence of scaffold material and architecture, especially pore size, strut size and surface/volume ratio on bone formation *in vivo* and to evaluate the mechanical properties of the resulting scaffolds and tissue constructs. Six groups of scaffolds, (three different designs and two different materials, PLLA and 50:50PLGA scaffolds) were fabricated. These scaffolds were seeded with transduced human gingival fibroblasts expressing BMP-7, and then implanted into mice subcutaneous pockets for 4 and 8 weeks. The scaffolds and scaffold/regenerated bone tissue construct were evaluated using Micro-computed tomography (μ-CT), mechanical testing, and histological assessments.

2. Methods

2.1. Porous Scaffold Design and Fabrication

Porous scaffolds 5mm in diameter and 3mm high with three different pore diameters (280, 550, and 820μm) were designed using image-based techniques (Fig 1, a). Based on the designed pore sizes, each group of the scaffolds was named Large (pore size = 820μm), Medium (pore size = 550μm), or Small (pore size = 280μm). First, the unit cells of each design were determined, and then, generated in a repeating pattern to fill the external scaffold geometry. The resulting image representations were converted to stereolithography (STL) formats and sliced in the Modelworks software (Solidscape, Inc., Merrimack, NH) to fabricate wax molds using a ModelMaker II (for Large and Medium) or PatternMaster™

(Fig 1, b) (for Small) 3D printer (Solidscape, Inc., Merrimack, NH). These wax molds (Fig 1, c) were cast into hydroxyapatite ceramic (HA) secondary molds (Fig 1, d). Polymer pellets, PLLA (Inherent Viscosity = 0.65dL/g) and 50:50PLGA (Inherent Viscosity = 0.61dL/g) (Birmingham Polymers Inc., AL), were heated at 205°C and 170 °C, respectively, in a Teflon mold. The HA molds were then placed into the Teflon mold containing molten polymer, in order to force the polymer through the open pore network. The HA molds were then removed from the porous polymer scaffolds using RDO Rapid Decalcifier (APEX Engineering Products Corp, Plainfield, IL). The scaffolds were sterilized in 70% ethanol overnight and then left in 100% ethanol until the day of implantation.

2.2. Cell preparation and scaffold implantation

Primary human gingival fibroblasts (HGFs) were prepared from explants of human surgical waste in compliance with the University of Michigan Institutional Review Board (Rutherford *et al.*, 1992). HGFs from passage 5- 10 were cultured near confluence in Alpha minimum essential medium (7agr;-MEM) supplemented with 10% fetal bovine serum, and 1% penicillin and streptomycin (Gibco). 24 hours before implantation, the HGFs were infected with AdCMV-BMP-7, a recombinant adenovirus construct expressing murine BMP-7 gene under a cytomegalovirus (CMV) promoter, at a multiplicity of infection (MOI) of 1000 PFU/cell (Franceschi *et al.*, 2000). Two million cells were seeded into each scaffold by suspending them in 60μl of 5mg/ml bovine plasma-derived fibrinogen (Sigma), and gelled with 6μl of 100U/ml bovine plasma-derived thrombin (Sigma). The scaffolds seeded with 2 million cells were subcutaneously implanted into immunocompromised mice (N: NIH-bg-nu-xid, Charles River, Wilmington, MA). After animals were anesthetized with an injection of ketamine/xylazine, 4 subcutaneous pockets were created and 4 scaffolds were implanted into each mouse, and finally surgical sites were closed with wound clips in compliance with University Committee on Use and Care of Animal (UCUCA) regulations. The mice were sacrificed at 4 and 8 weeks after the implantation, and the scaffold and tissue constructs were harvested, fixed with Z-fix (Anatech, Battle Creek, MI) and left in 70% ethanol for further assay.

2.3. Assay of scaffolds and regenerated tissues

All of the scaffolds pre-implantation alone and post-implantation with tissues were scanned using a MS-130 high resolution μ-CT Scanner (GE Medical Systems, Toronto, CAN) at a resolution of 16 μm. The scanned images were reconstructed using MicroView software (GE Healthcare). The reconstructed images were used to calculate the scaffold pore size, porosity and surface area prior to implantation and Bone volume (BV) and Tissue mineral density (TMD) were calculated for the scaffolds after implantation. The surfaces of pre-implanted scaffolds were also examined under a scanning electron microscope (XL30 ESEM, Philips). The environmental scanning electron microscopy (ESEM) mode was carried out at10kV and in a humid atmosphere of 0.7 Torr.

2.4. Mechanical test of scaffolds with regenerated tissue

Following μ-CT scanning, 4–7 replicates from each scaffold group were mechanically tested. Compression tests were performed after scaffolds were rehydrated for 30 minutes,

using a MTS Alliance RT30 Electromechanical test frame (MTS Systems Corp., MN). The cross head speed was 1mm/min after a preload of 0.227kg (0.5 lbs) for PLLA scaffolds and 0.0227kg (0.05 lbs) for 50:50PLGA scaffolds. The heights of the scaffolds were measured with a caliper, and the TestWorks4 software (MTS Systems Corp., MN) was used to record load and displacement data. The stress-strain curves were calculated from the initial dimensions of specimens. The compressive modulus was defined by the slope at the initial linear section of the stress-strain curve.

2.5. Histological analysis

After scanning with the μ-CT machine, one harvested scaffold from each group was also used for histological assay. The scaffold and tissue constructs were demineralized with RDO and the residual polymer in the tissue was removed using chloroform prior to paraffin-embedding. The scaffolds were then sectioned at 5 μm and stained with hematoxylin and eosin (H&E).

2.6. Statistical analysis

The statistical analysis was performed with SPSS (SPSS, Inc., Chicago, IL USA). Two groups were analyzed with Student's *t*-test for independent samples. Multiple comparison procedures were determined by one-way ANOVA followed by Tukey's Post Hoc multiple comparisons. Errors are reported in figures as the standard deviation (SD) and significance was determined using probability value of $p < 0.05$.

3. Results

3.1. Evaluation of the fabricated (pre-implanted) scaffolds

The schematics of the design and fabrication process of the scaffolds are depicted in Fig 1. HA secondary molds (Fig 1, d) ensured the fabrication process was identical between PLLA and 50:50PLGA scaffolds except for polymer casting temperatures. The architecture of the designs was the same for both the fabricated PLLA and 50:50PLGA scaffolds (Fig 1, e, f), which was also confirmed by μ-CT rendering images (Fig 2, a–f). The orthogonal pore locations and connections of the fabricated PLLA and 50:50PLGA scaffolds were also confirmed from the cross sectional images of μ-CT data (Fig 2, g–l). Low magnification ESEM images were similar in all groups (Fig 2, m–r), while the high magnification images showed slightly rougher surfaces on the PLLA scaffolds than the 50:50PLGA scaffolds (Fig 2, s–x, indicated by stars). Furthermore, porosity, surface to volume ratio, pore sizes and strut sizes were measured using the μ-CT images (Table 1). For each parameter, there was no significant difference between the fabricated PLLA and 50:50PLGA scaffolds. These data support the concept that the scaffold architectures within each design group (Large, Medium, and Small) made of the two materials are identical to each other. Porosity, pore size and strut size of the fabricated scaffolds decreased in order from Large to Small pore designs. The Small group had a higher surface to volume ratio than the Large and Medium group for both PLLA and 50:50PLGA scaffolds.

3.2. Histological observations of implanted scaffolds

Due to the secretion of BMP-7 from the transduced HGFs, all of the implanted scaffolds had bone-like tissue formation after 4 and 8 weeks (Fig 3). The histological images show cortical bone-like tissues formed outer layers and bone marrow-like tissues, such as trabecular structures, endothelial cells and osteoblasts, were observed within the cortical layer and the scaffolds. In the 4 week implant groups, most of the marrow-like tissues were distributed in the peripheral regions of the specimen. However, more bone marrow-like tissues containing blood vessel-like tissues were observed in the 8 week implants than in the 4 week implants. We found marrow- like tissue both at the center of the scaffolds and also in the surrounding regions at 8 weeks.

The histological images also show that tissue formation differed between PLLA and 50:50PLGA scaffold groups. After 4 weeks of implantation, little degradation of PLLA was observed, and most of their architectures remained intact (Fig 3, a–c). However, 50:50PLGA scaffolds degraded more rapidly and lost their initial architectures (Fig 3, d–f). After 8 weeks of implantation, PLLA scaffolds maintained their architecture, while most of 50:50PLGA degraded, leaving very little polymer, and the bone constructs appeared flattened (Fig 3, h–m). After degradation of most of the 50:50PLGA scaffolds, the histological images showed more bone marrow-like tissues containing blood vessel-like tissues in 8 week implants than in 4 week implants. For PLLA scaffolds, bone-like tissues formed mostly in the peripheral area of the scaffolds and very little bone ingrowth was observed (Fig 3, a–c, and g), and a few blood vessel-like tissues were seen inside of the scaffolds (Fig 3, g) at 4 weeks. At 8 weeks, advanced bone ingrowth was observed following the porous architectures of the Small PLLA scaffolds (Fig 3, j), and larger blood vessel tissues were also observed (Fig 3, n). In addition, there may be more fibrous tissue on PLLA scaffolds at 4 weeks than 8 weeks.

3.3. Tissue observations using μ-CT

Three dimensional tissue representations were generated from μ-CT data (Fig 4). Mineralized tissues were highlighted, and color contours indicated the density of the regenerated tissues. Highly dense tissues were distributed only on the outside of the scaffolds. Due to the rapid degradation, there was no bone growth into the 50:50PLGA scaffolds. All PLLA scaffolds maintained their architectures at all time points. There was some bone ingrowth into the PLLA scaffolds at 4 weeks, while there was slightly more bone ingrowth at 8 weeks. Maximum bone penetration was measured as the distance from the circular peripheral edge of each scaffold towards the center (N = 3–5 scaffolds). The bone penetration in the Small, Medium and Large PLLA scaffolds was 0.464 ± 0.024 mm, 0.723 ± 0.392 mm, and 0.457 ± 0.146 mm, respectively at 4 weeks, and 1.043 ± 0.292 mm, 0.834 ± 0.249 mm, and 0.773 ± 0.049 mm, respectively at 8 weeks. Small PLLA scaffolds supported a significant increase of bone penetration from 4 to 8 weeks. Large and Medium PLLA scaffolds also had increases in bone penetration, but these did not reach a statistically significant level. There was no significant difference between the scaffold groups at each time point. Also, the pattern of bone ingrowth followed the internal scaffold architectures, and bone tissues regenerated along the struts (Fig 4, g–i). More bone tissue distribution was

observed at 8 weeks than at 4 weeks with the highest amounts seen in the Small PLLA group, which had more bone surrounding the struts (Fig 4, i).

3.4. Tissue mineral density and bone volume of implanted scaffolds

TMD and BV were also calculated using μ-CT data (Fig 5, Table 2). The data demonstrated that TMD significantly increased in all groups from 4 week implantation to 8 weeks. From the 4 week implantation data, although there was no significant difference, the Small PLLA scaffold group had higher TMD than the Large and Medium PLLA scaffold groups (Fig 5, a). In addition, Large and Medium 50:50PLGA scaffold groups had more mineralized tissues than the Large and Medium of PLLA scaffold groups at 4 weeks (no significant difference). Medium and Small PLLA scaffold groups showed slightly higher mineral density than Medium and Small 50:50PLGA scaffold groups (Fig 5, b). The results of TMD were similar in all groups at both time points, while BV results showed different trends depending on the scaffold materials. Although only the Large 50:50PLGA showed a significant difference (Fig 5, c, d), the trends suggested that PLLA scaffolds lost their BV from 4 weeks to 8 weeks time points, while, 50:50PLGA increased BV during that time. In addition, other trends showed that PLLA scaffolds had more BV than 50:50PLGA scaffolds at the 4 weeks time point (Fig 5, c), however, after 8 weeks implantation, 50:50PLGA scaffolds showed higher BV (Fig 5, d) (no significant difference).

3.5. Mechanical properties

A compressive test was performed to investigate the changes in scaffold mechanical properties during implantation (Fig 6, a,d). The average mechanical properties of PLLA and 50:50PLGA scaffolds were equal to or greater than 100 MPa prior to implantation. All PLLA scaffolds had significantly decreased mechanical properties after 4 weeks of implantation due to polymer degradation (Fig 6, a). Then, their mechanical properties were increased or maintained after 8 weeks implantation due to growth of mineralized tissues. All 50:50PLGA scaffolds had nearly a complete loss of mechanical properties at 4 weeks, but then slightly increased after 8 weeks of implantation (Fig 6, b). The mechanical properties of all of the 50:50PLGA scaffolds were significantly lower than Small PLLA scaffolds at 4 weeks and Medium and Small PLLA scaffolds at 8 weeks.

The correlation between the modulus and bone volume are shown in Fig 6 (b, c, e, f). PLLA scaffolds did not have any correlation at 4 ($R^2 = 0.0371$) and 8 ($R^2 = 0.0102$) weeks. However, 50:50PLGA scaffolds had some correlation at 4 ($R^2 = 0.4809$) and 8 ($R^2 = 0.4043$) weeks. The 8 week data had an outlier which lowered the correlation, which increased to $R^2 = 0.8884$ without the outlier. These results indicate that increased bone deposition increased the moduli of the regenerated tissues when the scaffold modulus was significantly reduced.

4. Discussion

Computer based scaffold design and SFF were used to determine the effect of porous scaffold material and architecture on bone regeneration. PLLA and 50:50PLGA scaffolds were fabricated using the identical procedure with the exception of their melting

temperatures. The semi-crystalline structure of PLLA required a higher casting temperature, while the 50:50PLGA can be melted at a lower temperature than PLLA due to its amorphous structure. The μ-CT data demonstrated that the fabricated PLLA and 50:50PLGA scaffolds had similar defined pore sizes, strut sizes, porosities and surface to volume ratios. In addition, the μ-CT results verified that the fabricated scaffolds in the same design groups had identical internal and external architectures between materials. Although the viscosities of the polymers were similar, the surface morphologies of the scaffolds were slightly different as shown in the ESEM images. This may be due to the difference of the chemical structures including crystallinity of the polymers.

Ex vivo gene therapy was used to induce bone formation from the surrounding tissues at the implant site. This regenerative gene therapy strategy using adenoviral vectors can be applied to transduce various cells, such as bone marrow stromal cells (Chang *et al.*, 2003), and fibroblasts(Krebsbach *et al.*, 2000, Hirata *et al.*, 2003). The consistent secretion of BMP-2 from adenovirus transduced HGFs up to 2 weeks *in vitro* has been reported (Shin *et al.*, 2010). Additionally, this approach has been studied to induce endochondral-like bone tissue formation by transduced HGFs (Krebsbach *et al.*, 2000, Rutherford *et al.*, 2002). Other methods of bone formation have previously been reported, including seeding bone marrow stromal cells (Claase *et al.*, 2007), incorporation of BMP-7 into nanospheres (Wei *et al.*, 2007), and BMP-2 conjugated with heparin (Claase *et al.*, 2007). However, these methods require pre-treatment of the scaffolds prior to implantation. The scaffolds may start degrading during the preparation, especially 50:50PLGA scaffolds due to their short degradation profile. Therefore, to minimize any alteration of the scaffolds before implantation and successfully regenerate bone tissue *in vivo*, *ex vivo* gene therapy was a suitable method for testing this study.

Scaffold tissue constructs differed between the PLLA and 50:50PLGA scaffolds due to polymer degradation. PLLA scaffolds maintained their architecture throughout the study period, while 50:50PLGA scaffolds completely lost the original designed pore structure, and there were only chunks remaining at the 4 week time point. The hydrophilicity of the PGA component in PLGA may induce faster water uptake and hydrolysis leading to faster degradation (Lu *et al.*, 2000). In contrast, the methyl group of the PLLA side chain contributes to the hydrophobicity of the polymer, resulting in slower degradation (Ishaug-Riley *et al.*, 1999). As reported previously, the *in vivo* half-life of 50:50PLGA foams was about 2 weeks (Lu *et al.*, 2000), our 50:50PLGA scaffolds may maintain their architectures for only a few weeks or less *in vivo*.

Due to the rapid degradation, little bone tissue was found inside the degraded 50:50PLGA scaffolds at 4 and 8 weeks. In contrast, the PLLA scaffolds had small amounts of bone ingrowth and some blood vessel-like tissues from the histological analysis. These differences may be attributed to the effects of degradation by-products on cell activities. PLLA nanofibers or porous membranes supported activities of chondrocytes and human mesenchymal stem cells and vascularization more than those of 50:50PLGA since rapid degradation of 50:50PLGA created acidic environments and prevented cell activities on or in the constructs (Li *et al.*, 2006, Kaushiva *et al.*, 2007). In addition, reduction of pH negatively affected activities of bone marrow stromal cells during osteogenesis (Kohn *et al.*,

2002). Although there are no data regarding pH change or acidic by-products in this study, there may be similar effects on cell activities and tissue formation for both the PLLA and 50:50PLGA scaffolds at the earlier time point. Additionally, the collapse of the PLGA porous architecture would prohibit cell migration and bone formation within the scaffold interior.

The trends of BV results show that BV was higher on the PLLA scaffolds than the 50:50PLGA scaffolds at 4 weeks, while the 50:50PLGA scaffolds had higher BV at 8 weeks. The acidic environment may also explain the change in bone volume over time. Initially, at 4 weeks, bone formation was inhibited by more acidic by-products in the environment on the PLGA scaffolds, but, the removal of these degradation by-products allowed restoration of cellular activities which may have led to the bone volume increase observed at the 8 week time point. The PLLA scaffolds may have more degradation by-products which may lower BV at 8 weeks. From the data shown in this and previous studies (Li *et al.*, 2006, Kaushiva *et al.*, 2007, Kohn *et al.*, 2002), PLLA scaffolds may be more useful in this situation because it has a slower degradation rate that allows new tissue to generate while it still maintaining sufficient mechanical properties to support new tissue growth. In comparison, the 50:50PLGA is not able to support the tissue due to its fast degradation profile. It would be useful to study another polymer, such as 85:15PLGA that lasts longer *in vivo*, as SFF scaffolds for bone application. Furthermore, the effects of SFF scaffolds on degradation need to be investigated to better understand the interaction between scaffolds and tissue formation.

The PLLA scaffolds in this study showed much less bone ingrowth than porous HA scaffolds and porous poly (propylene fumerate)/tricalcium phosphate (PPF/TCP) scaffolds reported in our previous studies (Schek *et al.*, 2006, Lin *et al.*, 2005) since HA and TCP are known osteoconductive materials that have been shown to allow chemotactic adherence for enhanced bone growth. Furthermore, hydrophobic materials, like PLLA, may delay cell attachment and bone formation (Oh *et al.*, 2007, Oh *et al.*, 2003). In addition, the layers of tissues or bony shell surrounding the PLLA scaffolds prevent diffusion of nutrients into the construct (Kruyt *et al.*, 2007) and may cause accumulation of acidic by-product inside of the implants, which could prohibit cell migration and tissue ingrowth.

The importance of scaffolds pore sizes for bone formation has been discussed in many studies. The minimum pore size, 280 μm, in this study was chosen based on the required diameters for blood vessel formation, which was approximated according to *in vivo* bone tissue formation in previous studies (Kuboki *et al.*, 2001, Oh *et al.*, 2007, Druecke *et al.*, 2004). Although the effect of pore size of PLLA or PLGA porous scaffolds on bone regeneration has been explored in various studies, these results varied depending on the materials and methods of the study. For example, pore sizes of PLGA scaffolds did not affect osteoblast activities *in vitro* nor was *in vivo* bone formation influenced by pore sizes within the range of 150–710 μm and 125–500 μm (Ishaug-Riley *et al.*, 1997, Ishaug-Riley *et al.*, 1998, Wu *et al.*, 2006). In contrast, another group compared porous PLGA scaffolds with constant porosity and indicated that pore size between 400 and 600 μm were favorable for osteoblasts rather than 300 μm or smaller pore sizes (Pamula *et al.*, 2008a, Pamula *et al.*, 2008b). Another study demonstrated that PLLA scaffolds with pores of 350 μm diameters

induced more bone ingrowth than the smaller ones (100 and 200 μm) when implanted in rabbits' calvarias (Robinson *et al.*, 1995). However, it is again critical to note that these previous studies, which suggested an influence of pore diameter (Pamula *et al.*, 2008a, Pamula *et al.*, 2008b, Robinson *et al.*, 1995), utilized conventional fabrication techniques which did not rigorously control pore diameter and interconnectivity. Our chosen pore size, 280, 550 and 820 μm, thus bracketed the range of pore sizes investigated in previous studies: with the difference being the controlled interconnected, repeatable architecture in this study. The pore range is also within the range of the reported trabecular pore sizes, 300 ~ 1000 μm (Keaveny *et al.*, 2001, Rezwan *et al.*, 2006).

Regarding bone ingrowth from μ-CT images, we did not observe any significant difference between the scaffolds designs, such as pore size, which is in agreement with our previous studies (Schek *et al.*, 2006, Roosa *et al.*, 2010). The distances of bone penetration into the PLLA scaffolds in this study was more than previously reported in PLGA foams implanted in the rat mesentery for 49 days (Ishaug-Riley *et al.*, 1997). The distances generally increased from 4 to 8 weeks in our study, while the previous study showed that there was little increase over the implantation time. This may be due to their use of foam scaffolds, which have random oriented pores and non-controlled internal architectures, and a more tortuous pathway that may prevent nutrient diffusion and cell migration into the scaffolds (Melchels *et al.*, 2010). Silva et al. demonstrated that porous HA and PLLA scaffolds with aligned channels could improve cell infiltration into the center of the scaffolds (Silva *et al.*, 2006). Their study and our results indicate that orthogonally interconnected porous architectures may not only help increase nutrient diffusion when compared to foam scaffolds, but may also guide tissue ingrowth.

Other scaffold design parameters, such as porosity and surface area, did not seem to have a significant effect on bone formation in this study. Although high porosity has been discussed as an important requirement of scaffolds (Sosnowski *et al.*, 2006), the effect of scaffold porosity on bone formation was not significant in this study. Since our scaffolds have fully and orthogonally interconnected pore architectures or channels, infiltration of nutrients into the scaffolds may not be different between the scaffold design groups. The pore sizes of the scaffolds varied the surface areas of the scaffolds onto which cells from host tissue can attach. The μ-CT data also showed that the patterns of bone ingrowth followed the internal architectures of the scaffolds. Small PLLA scaffolds had the smallest strut sizes and pore sizes which allowed the tissues to surround the struts and interlock, increasing tissue integration. This may help to form stronger bonds between the regenerated tissues and porous scaffolds. The scaffolds with smaller pores had more total surface area than the scaffolds with larger pores, which may create a larger surface area for cell adhesion and help bone formation. Furthermore, another scaffold design parameter may have a more impactful factor on increasing bone formation. For example, it has been postulated that pore interconnectivity and permeability may be an important scaffold design parameters (Melchels *et al.*, 2010, Hui *et al.*, 1996, Jones *et al.*, 2009).

For functional use of these scaffolds at load bearing sites, it is important to understand the time dependent changes in scaffold/tissue construct mechanical properties. Initially, the fabricated PLLA and 50:50PLGA scaffolds had mechanical properties in the low to medium

range of human trabecular bone (Saito *et al.*, 2010). After implantation, the mechanical properties decreased due to the degradation of materials. As shown in the histology and μ-CT images, 50:50PLGA scaffolds completely lost their designed architectures, and their mechanical properties decreased dramatically both at 4 and 8 weeks compared with the pre-implanted scaffolds and the PLLA scaffolds. Despite the retention of designed architecture, PLLA scaffolds also showed a decrease in their mechanical properties, which indicates some polymer degradation.

The mechanical properties of PLLA scaffolds with bone tissue were significantly higher than those of 50:50PLGA scaffolds at 4 and 8 weeks. There was no correlation between bone volume and PLLA/bone construct mechanical properties at 4 and 8 weeks. However, the 50:50PLGA/bone construct mechanical properties showed some correlation with bone volume at 4 weeks, which increased at 8 weeks. The mechanical properties of the PLLA scaffold constructs, due to the greater retention of polymer architecture and mechanical properties, were likely more dependent on the polymer at 4 and 8 weeks. In contrast, the 50:50PLGA mechanical properties were solely dependent on the generated bone as the polymer was degraded by 4 weeks.

Although, the majority of PLLA mechanical properties relied on the scaffold material, Large and Medium PLLA scaffolds still exhibited an increasing trend in mechanical properties due to higher mineralized tissues and bone growth on/into the scaffolds from 4 to 8 weeks. Small PLLA scaffolds had similar mechanical properties at both time points. Small PLLA scaffolds may have a slower degradation speed, maintaining their mechanical properties longer than the other groups.

One of the limitations in this study is that ectopic sites do not provide the same environment as orthotopic sites, including mechanical stimulation, nutrients, cell types and cell-cell interactions. For example, the bone volume of PLLA scaffolds decreased from 4 to 8 weeks, similar to findings by Lin et al. (Lin *et al.*, 2005). This may because there is little loading on the ectopic models to simulate bone remodeling and increases in mineralization of newly formed tissues (Duty *et al.*, 2007) as well as less nutrient supply. In addition, mechanical loading on the scaffolds would increase the degradation of PLLA scaffolds in terms of molecular weight and mechanical properties (Kang *et al.*, 2009).

5. Conclusions

In the present study, we compared the effect of materials and architectures of porous scaffolds on bone formation. Our data demonstrated that material choice significantly influences *in vivo* bone tissue regeneration and mechanical properties. We also found that scaffold architecture controls the patterns of bone ingrowth and mechanical properties of scaffold-bone constructs. The 50:50PLGA scaffolds degraded rapidly, providing little initial support for bone ingrowth, and had very low mechanical properties. In comparison, the PLLA scaffolds maintained their architectures throughout the study period and supported some blood vessel and bone ingrowth. Given the long tissue regeneration time seen in many clinical applications (e.g. spine fusion, long bone defects, mandibular defects) the ability of a polymer scaffold to maintain structural and mechanical properties up to 6 month is critical.

Pore size, if architecture is maintained and does not collapse, does not significantly influence bone regeneration. The patterns of bone tissue ingrowth were defined by the computer designed pores and struts of the scaffolds. Furthermore, mechanical properties of implanted scaffolds can be controlled by the initial architectures. All of these results support the importance of choosing suitable scaffold materials and designing conductive scaffold architectures that are ideal for bone tissue regeneration. Each of these factors will need to be fine tuned in order to find the desired properties for specific anatomical sites or defects.

Acknowledgments

This study was supported by National Institute of Health (NIH) R01 grant AR 053379.

References

Athanasiou KA, Agrawal CM, Barber FA, Burkhart SS. Orthopaedic applications for PLA-PGA biodegradable polymers. Arthroscopy. 1998; 14:726–37. [PubMed: 9788368]

Bessa PC, Casal M, Reis RL. Bone morphogenetic proteins in tissue engineering: the road from laboratory to clinic, part II (BMP delivery). J Tissue Eng Regen Med. 2008a; 2:81–96. [PubMed: 18383454]

Bessa PC, Casal M, Reis RL. Bone morphogenetic proteins in tissue engineering: the road from the laboratory to the clinic, part I (basic concepts). J Tissue Eng Regen Med. 2008b; 2:1–13. [PubMed: 18293427]

Cao Y, Mitchell G, Messina A, Price L, Thompson E, Penington A, Morrison W, O'Connor A, Stevens G, Cooper-White J. The influence of architecture on degradation and tissue ingrowth into three-dimensional poly(lactic-co-glycolic acid) scaffolds in vitro and in vivo. Biomaterials. 2006; 27:2854–64. [PubMed: 16426678]

Chang SC, Chuang HL, Chen YR, Chen JK, Chung HY, Lu YL, Lin HY, Tai CL, Lou J. Ex vivo gene therapy in autologous bone marrow stromal stem cells for tissue-engineered maxillofacial bone regeneration. Gene Ther. 2003; 10:2013–9. [PubMed: 14566360]

Claase MB, de Bruijn JD, Grijpma DW, Feijen J. Ectopic bone formation in cell-seeded poly(ethylene oxide)/poly(butylene terephthalate) copolymer scaffolds of varying porosity. J Mater Sci Mater Med. 2007; 18:1299–307. [PubMed: 17268874]

Druecke D, Langer S, Lamme E, Pieper J, Ugarkovic M, Steinau HU, Homann HH. Neovascularization of poly(ether ester) block-copolymer scaffolds in vivo: long-term investigations using intravital fluorescent microscopy. J Biomed Mater Res A. 2004; 68:10–8. [PubMed: 14661244]

Duty AO, Oest ME, Guldberg RE. Cyclic mechanical compression increases mineralization of cell-seeded polymer scaffolds in vivo. J Biomech Eng. 2007; 129:531–9. [PubMed: 17655474]

Franceschi RT, Wang D, Krebsbach PH, Rutherford RB. Gene therapy for bone formation: in vitro and in vivo osteogenic activity of an adenovirus expressing BMP7. J Cell Biochem. 2000; 78:476–86. [PubMed: 10861845]

Goldstein AS, Zhu G, Morris GE, Meszlenyi RK, Mikos AG. Effect of osteoblastic culture conditions on the structure of poly(DL-lactic-co-glycolic acid) foam scaffolds. Tissue Eng. 1999; 5:421–34. [PubMed: 10586098]

Gomes ME, Holtorf HL, Reis RL, Mikos AG. Influence of the porosity of starch-based fiber mesh scaffolds on the proliferation and osteogenic differentiation of bone marrow stromal cells cultured in a flow perfusion bioreactor. Tissue Eng. 2006; 12:801–9. [PubMed: 16674293]

Hirata K, Tsukazaki T, Kadowaki A, Furukawa K, Shibata Y, Moriishi T, Okubo Y, Bessho K, Komori T, Mizuno A, Yamaguchi A. Transplantation of skin fibroblasts expressing BMP-2 promotes bone repair more effectively than those expressing Runx2. Bone. 2003; 32:502–12. [PubMed: 12753866]

Hollister SJ. Porous scaffold design for tissue engineering. Nat Mater. 2005; 4:518–24. [PubMed: 16003400]

Hollister SJ, Levy RA, Chu TM, Halloran JW, Feinberg SE. An image-based approach for designing and manufacturing craniofacial scaffolds. Int J Oral Maxillofac Surg. 2000; 29:67–71. [PubMed: 10691148]

Hollister SJ, Maddox RD, Taboas JM. Optimal design and fabrication of scaffolds to mimic tissue properties and satisfy biological constraints. Biomaterials. 2002; 23:4095–103. [PubMed: 12182311]

Hsu SH, Yen HJ, Tseng CS, Cheng CS, Tsai CL. Evaluation of the growth of chondrocytes and osteoblasts seeded into precision scaffolds fabricated by fused deposition manufacturing. J Biomed Mater Res B Appl Biomater. 2007; 80:519–27. [PubMed: 16862556]

Hui PW, Leung PC, Sher A. Fluid conductance of cancellous bone graft as a predictor for graft-host interface healing. J Biomech. 1996; 29:123–32. [PubMed: 8839025]

Hutmacher DW. Scaffold design and fabrication technologies for engineering tissues--state of the art and future perspectives. J Biomater Sci Polym Ed. 2001; 12:107–24. [PubMed: 11334185]

Hutmacher DW, Schantz T, Zein I, Ng KW, Teoh SH, Tan KC. Mechanical properties and cell cultural response of polycaprolactone scaffolds designed and fabricated via fused deposition modeling. J Biomed Mater Res. 2001; 55:203–16. [PubMed: 11255172]

Hutmacher DW, Sittinger M, Risbud MV. Scaffold-based tissue engineering: rationale for computer-aided design and solid free-form fabrication systems. Trends Biotechnol. 2004; 22:354–62. [PubMed: 15245908]

Ishaug-Riley SL, Crane GM, Gurlek A, Miller MJ, Yasko AW, Yaszemski MJ, Mikos AG. Ectopic bone formation by marrow stromal osteoblast transplantation using poly(DL-lactic-co-glycolic acid) foams implanted into the rat mesentery. J Biomed Mater Res. 1997; 36:1–8. [PubMed: 9212383]

Ishaug-Riley SL, Crane-Kruger GM, Yaszemski MJ, Mikos AG. Three-dimensional culture of rat calvarial osteoblasts in porous biodegradable polymers. Biomaterials. 1998; 19:1405–12. [PubMed: 9758040]

Ishaug-Riley SL, Okun LE, Prado G, Applegate MA, Ratcliffe A. Human articular chondrocyte adhesion and proliferation on synthetic biodegradable polymer films. Biomaterials. 1999; 20:2245–56. [PubMed: 10614931]

Jones AC, Arns CH, Hutmacher DW, Milthorpe BK, Sheppard AP, Knackstedt MA. The correlation of pore morphology, interconnectivity and physical properties of 3D ceramic scaffolds with bone ingrowth. Biomaterials. 2009; 30:1440–51. [PubMed: 19091398]

Kang Y, Yao Y, Yin G, Huang Z, Liao X, Xu X, Zhao G. A study on the in vitro degradation properties of poly(L-lactic acid)/beta-tricalcuim phosphate (PLLA/beta-TCP) scaffold under dynamic loading. Med Eng Phys. 2009; 31:589–94. [PubMed: 19131266]

Karageorgiou V, Kaplan D. Porosity of 3D biomaterial scaffolds and osteogenesis. Biomaterials. 2005; 26:5474–91. [PubMed: 15860204]

Kaushiva A, Turzhitsky VM, Darmoc M, Backman V, Ameer GA. A biodegradable vascularizing membrane: a feasibility study. Acta Biomater. 2007; 3:631–42. [PubMed: 17507300]

Keaveny TM, Morgan EF, Niebur GL, Yeh OC. Biomechanics of trabecular bone. Annu Rev Biomed Eng. 2001; 3:307–33. [PubMed: 11447066]

Khan Y, Yaszemski MJ, Mikos AG, Laurencin CT. Tissue engineering of bone: material and matrix considerations. J Bone Joint Surg Am. 2008; 90(Suppl 1):36–42. [PubMed: 18292355]

Kohn DH, Sarmadi M, Helman JI, Krebsbach PH. Effects of pH on human bone marrow stromal cells in vitro: implications for tissue engineering of bone. J Biomed Mater Res. 2002; 60:292–9. [PubMed: 11857436]

Kontakis GM, Pagkalos JE, Tosounidis TI, Melissas J, Katonis P. Bioabsorbable materials in orthopaedics. Acta Orthop Belg. 2007; 73:159–69. [PubMed: 17515225]

Krebsbach PH, Gu K, Franceschi RT, Rutherford RB. Gene therapy-directed osteogenesis: BMP-7-transduced human fibroblasts form bone in vivo. Hum Gene Ther. 2000; 11:1201–10. [PubMed: 10834621]

Kruyt MC, Dhert WJ, Oner FC, van Blitterswijk CA, Verbout AJ, de Bruijn JD. Analysis of ectopic and orthotopic bone formation in cell-based tissue-engineered constructs in goats. Biomaterials. 2007; 28:1798–805. [PubMed: 17182096]

Kuboki Y, Jin Q, Takita H. Geometry of carriers controlling phenotypic expression in BMP-induced osteogenesis and chondrogenesis. J Bone Joint Surg Am. 2001; 83-A(Suppl 1):S105–15. [PubMed: 11314788]

Li JP, Habibovic P, van den Doel M, Wilson CE, de Wijn JR, van Blitterswijk CA, de Groot K. Bone ingrowth in porous titanium implants produced by 3D fiber deposition. Biomaterials. 2007; 28:2810–20. [PubMed: 17367852]

Li WJ, Cooper JA Jr, Mauck RL, Tuan RS. Fabrication and characterization of six electrospun poly(alpha-hydroxy ester)-based fibrous scaffolds for tissue engineering applications. Acta Biomater. 2006; 2:377–85. [PubMed: 16765878]

Lin CY, Kikuchi N, Hollister SJ. A novel method for biomaterial scaffold internal architecture design to match bone elastic properties with desired porosity. J Biomech. 2004; 37:623–36. [PubMed: 15046991]

Lin CY, Schek RM, Mistry AS, Shi X, Mikos AG, Krebsbach PH, Hollister SJ. Functional bone engineering using ex vivo gene therapy and topology-optimized, biodegradable polymer composite scaffolds. Tissue Eng. 2005; 11:1589–98. [PubMed: 16259612]

Lu L, Peter SJ, Lyman MD, Lai HL, Leite SM, Tamada JA, Uyama S, Vacanti JP, Langer R, Mikos AG. In vitro and in vivo degradation of porous poly(DL-lactic-co-glycolic acid) foams. Biomaterials. 2000; 21:1837–45. [PubMed: 10919687]

Martins A, Chung S, Pedro AJ, Sousa RA, Marques AP, Reis RL, Neves NM. Hierarchical starch-based fibrous scaffold for bone tissue engineering applications. J Tissue Eng Regen Med. 2009; 3:37–42. [PubMed: 19021239]

Melchels FP, Barradas AM, van Blitterswijk CA, de Boer J, Feijen J, Grijpma DW. Effects of the architecture of tissue engineering scaffolds on cell seeding and culturing. Acta Biomater. 2010; 6:4208–17. [PubMed: 20561602]

Middleton JC, Tipton AJ. Synthetic biodegradable polymers as orthopedic devices. Biomaterials. 2000; 21:2335–46. [PubMed: 11055281]

Narayan D, Venkatraman SS. Effect of pore size and interpore distance on endothelial cell growth on polymers. J Biomed Mater Res A. 2008; 87:710–8. [PubMed: 18200559]

Nussenbaum B, Krebsbach PH. The role of gene therapy for craniofacial and dental tissue engineering. Adv Drug Deliv Rev. 2006; 58:577–91. [PubMed: 16766080]

Oh SH, Kang SG, Kim ES, Cho SH, Lee JH. Fabrication and characterization of hydrophilic poly(lactic-co-glycolic acid)/poly(vinyl alcohol) blend cell scaffolds by melt-molding particulate-leaching method. Biomaterials. 2003; 24:4011–21. [PubMed: 12834596]

Oh SH, Park IK, Kim JM, Lee JH. In vitro and in vivo characteristics of PCL scaffolds with pore size gradient fabricated by a centrifugation method. Biomaterials. 2007; 28:1664–71. [PubMed: 17196648]

Pamula E, Bacakova L, Filova E, Buczynska J, Dobrzynski P, Noskova L, Grausova L. The influence of pore size on colonization of poly(L-lactide-glycolide) scaffolds with human osteoblast-like MG 63 cells in vitro. J Mater Sci Mater Med. 2008a; 19:425–35. [PubMed: 17607515]

Pamula E, Filova E, Bacakova L, Lisa V, Adamczyk D. Resorbable polymeric scaffolds for bone tissue engineering: The influence of their microstructure on the growth of human osteoblast-like MG 63 cells. J Biomed Mater Res A. 2008b

Rezwan K, Chen QZ, Blaker JJ, Boccaccini AR. Biodegradable and bioactive porous polymer/inorganic composite scaffolds for bone tissue engineering. Biomaterials. 2006; 27:3413–31. [PubMed: 16504284]

Robinson BP, Hollinger JO, Szachowicz EH, Brekke J. Calvarial bone repair with porous D, L-polylactide. Otolaryngol Head Neck Surg. 1995; 112:707–13. [PubMed: 7777356]

Roosa SM, Kemppainen JM, Moffitt EN, Krebsbach PH, Hollister SJ. The pore size of polycaprolactone scaffolds has limited influence on bone regeneration in an in vivo model. J Biomed Mater Res A. 2010; 92:359–68. [PubMed: 19189391]

Rose FR, Cyster LA, Grant DM, Scotchford CA, Howdle SM, Shakesheff KM. In vitro assessment of cell penetration into porous hydroxyapatite scaffolds with a central aligned channel. Biomaterials. 2004; 25:5507–14. [PubMed: 15142732]

Rutherford RB, Moalli M, Franceschi RT, Wang D, Gu K, Krebsbach PH. Bone morphogenetic protein-transduced human fibroblasts convert to osteoblasts and form bone in vivo. Tissue Eng. 2002; 8:441–52. [PubMed: 12167230]

Rutherford RB, TrailSmith MD, Ryan ME, Charette MF. Synergistic effects of dexamethasone on platelet-derived growth factor mitogenesis in vitro. Arch Oral Biol. 1992; 37:139–45. [PubMed: 1622340]

Saito E, Kang H, Taboas JM, Diggs A, Flanagan CL, Hollister SJ. Experimental and computational characterization of designed and fabricated 50:50 PLGA porous scaffolds for human trabecular bone applications. J Mater Sci Mater Med. 2010; 21:2371–83. [PubMed: 20524047]

Schek RM, Wilke EN, Hollister SJ, Krebsbach PH. Combined use of designed scaffolds and adenoviral gene therapy for skeletal tissue engineering. Biomaterials. 2006; 27:1160–6. [PubMed: 16112727]

Shin JH, Kim KH, Kim SH, Koo KT, Kim TI, Seol YJ, Ku Y, Rhyu IC, Chung CP, Lee YM. Ex vivo bone morphogenetic protein-2 gene delivery using gingival fibroblasts promotes bone regeneration in rats. J Clin Periodontol. 2010; 37:305–11. [PubMed: 20041973]

Silva MM, Cyster LA, Barry JJ, Yang XB, Oreffo RO, Grant DM, Scotchford CA, Howdle SM, Shakesheff KM, Rose FR. The effect of anisotropic architecture on cell and tissue infiltration into tissue engineering scaffolds. Biomaterials. 2006; 27:5909–17. [PubMed: 16949666]

Sinha RK, Morris F, Shah SA, Tuan RS. Surface composition of orthopaedic implant metals regulates cell attachment, spreading, and cytoskeletal organization of primary human osteoblasts in vitro. Clin Orthop Relat Res. 1994; (305):258–72. [PubMed: 8050238]

Sosnowski S, Wozniak P, Lewandowska-Szumiel M. Polyester scaffolds with bimodal pore size distribution for tissue engineering. Macromol Biosci. 2006; 6:425–34. [PubMed: 16761274]

Sun W, Starly B, Darling A, Gomez C. Computer-aided tissue engineering: application to biomimetic modelling and design of tissue scaffolds. Biotechnol Appl Biochem. 2004; 39:49–58. [PubMed: 14556653]

Taboas JM, Maddox RD, Krebsbach PH, Hollister SJ. Indirect solid free form fabrication of local and global porous, biomimetic and composite 3D polymer-ceramic scaffolds. Biomaterials. 2003; 24:181–94. [PubMed: 12417192]

Tsuruga E, Takita H, Itoh H, Wakisaka Y, Kuboki Y. Pore size of porous hydroxyapatite as the cell-substratum controls BMP-induced osteogenesis. J Biochem. 1997; 121:317–24. [PubMed: 9089406]

Wei G, Jin Q, Giannobile WV, Ma PX. The enhancement of osteogenesis by nano-fibrous scaffolds incorporating rhBMP-7 nanospheres. Biomaterials. 2007; 28:2087–96. [PubMed: 17239946]

Williams JM, Adewunmi A, Schek RM, Flanagan CL, Krebsbach PH, Feinberg SE, Hollister SJ, Das S. Bone tissue engineering using polycaprolactone scaffolds fabricated via selective laser sintering. Biomaterials. 2005; 26:4817–27. [PubMed: 15763261]

Wu YC, Shaw SY, Lin HR, Lee TM, Yang CY. Bone tissue engineering evaluation based on rat calvaria stromal cells cultured on modified PLGA scaffolds. Biomaterials. 2006; 27:896–904. [PubMed: 16125224]

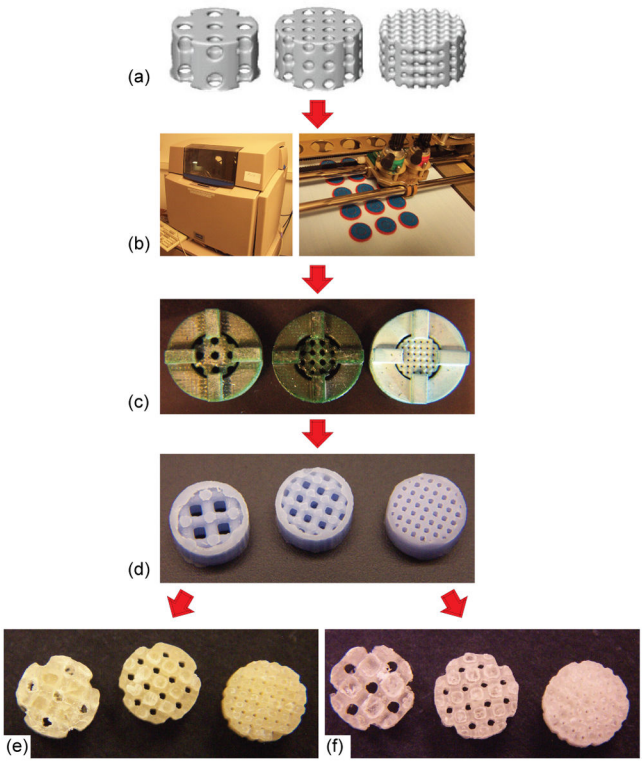

Figure 1.

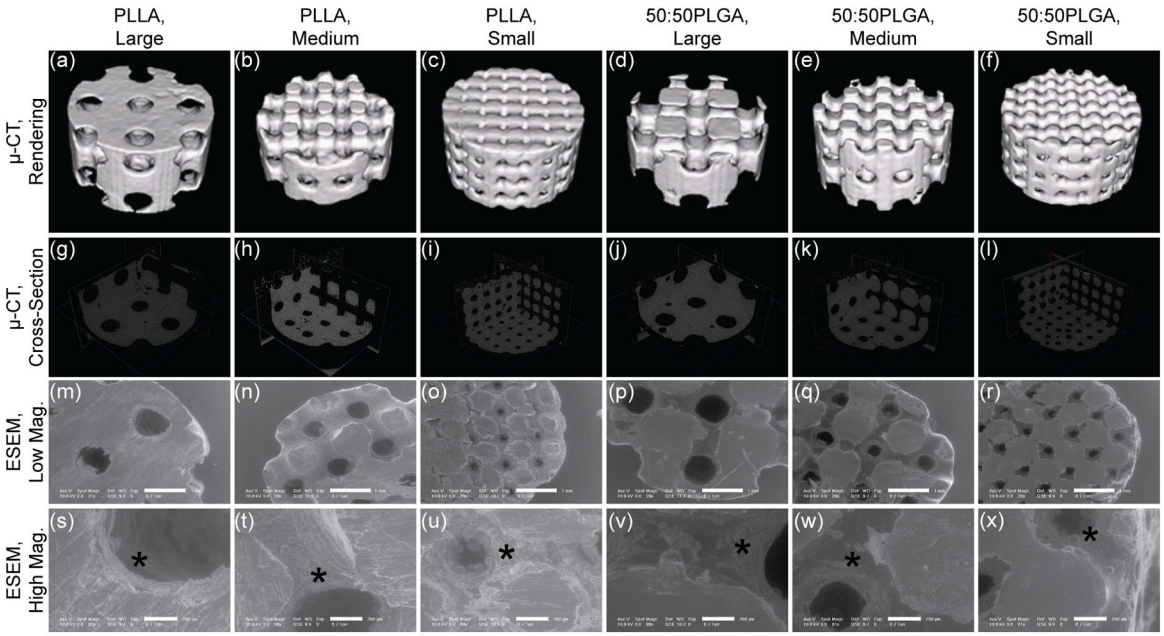

Figure 2.

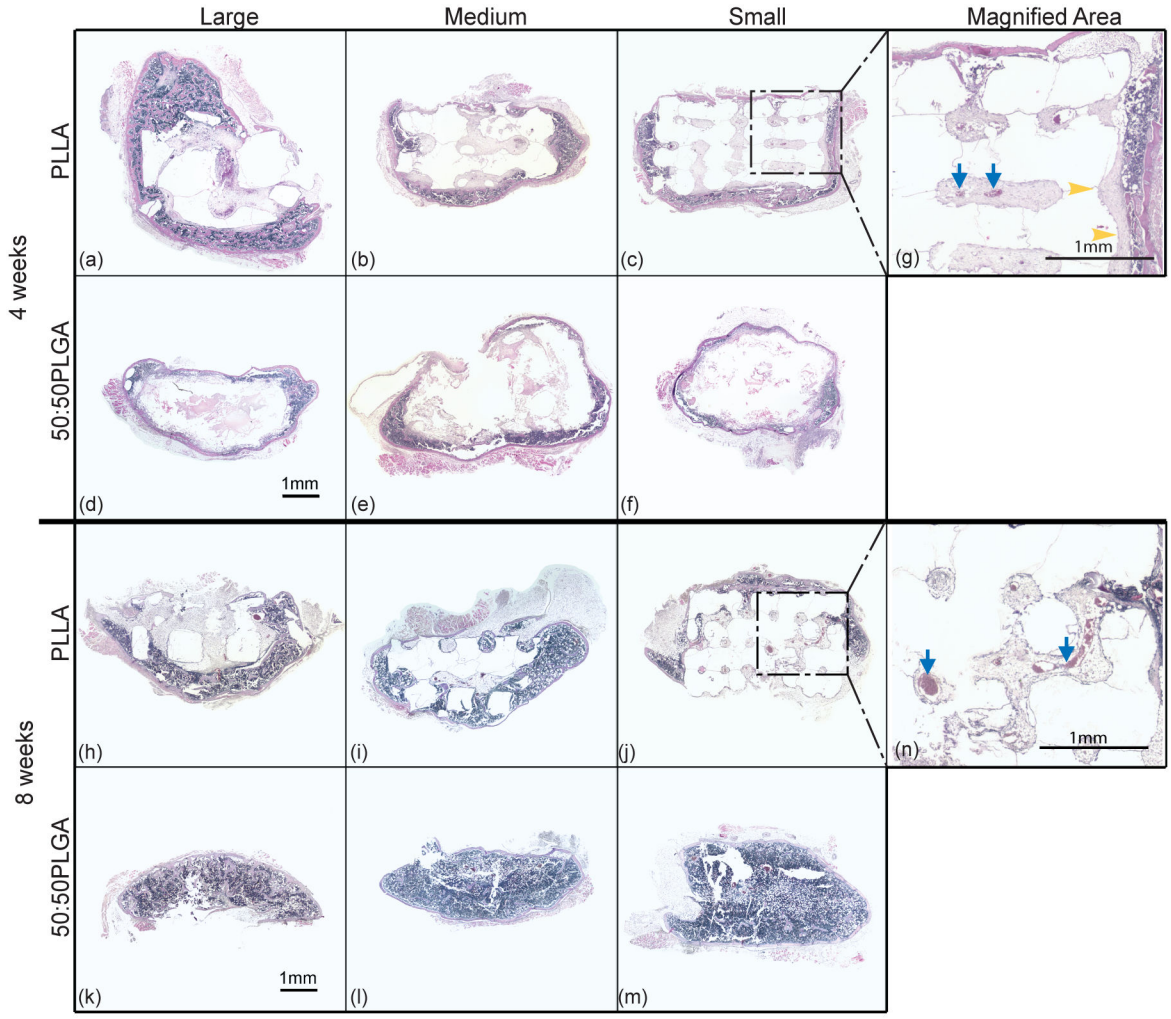

Figure 3.

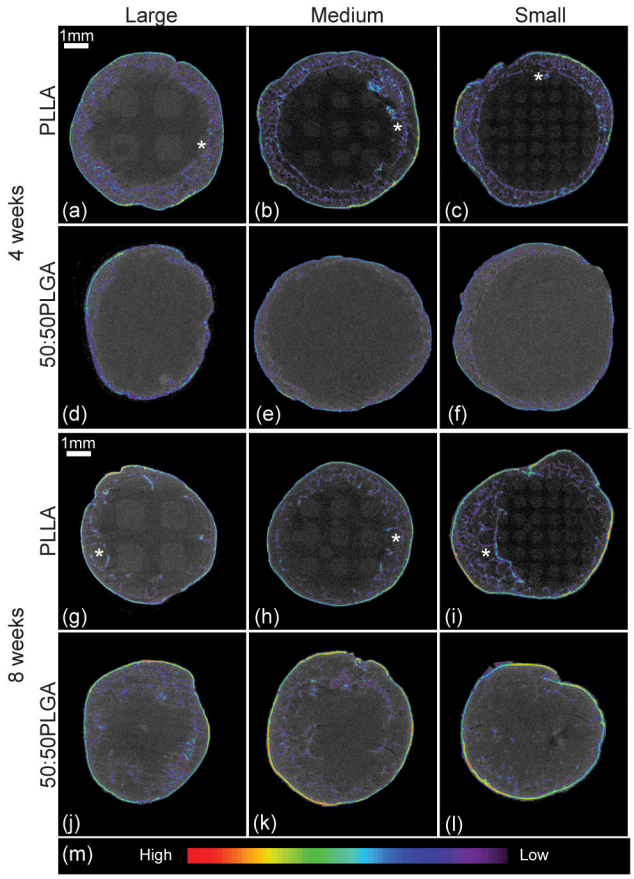

Figure 4.

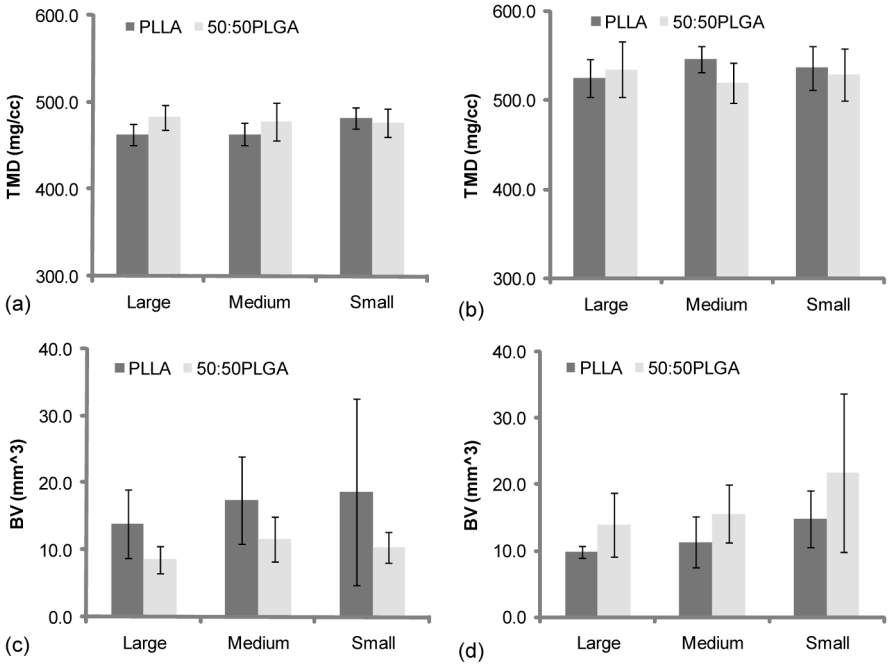

Figure 5.

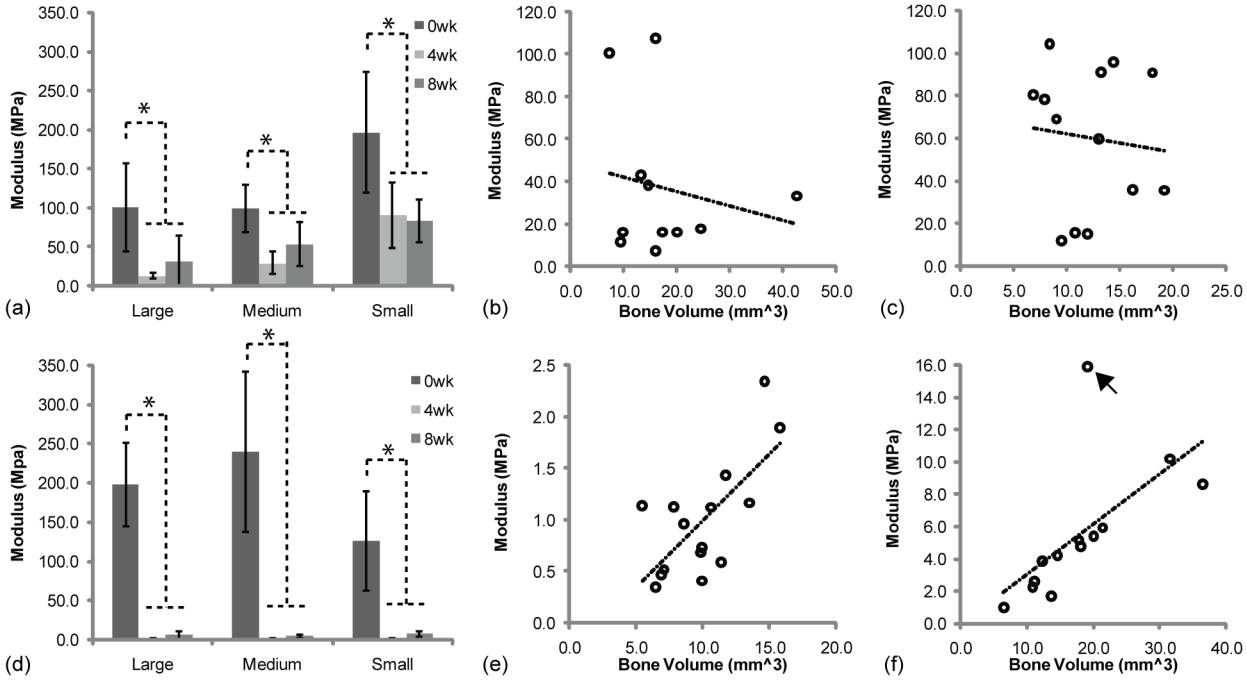

Figure 6.

Table 1

Fabricated scaffold dimensions

	PLLA			50:50PLGA		
	Large	**Medium**	**Small**	**Large**	**Medium**	**Small**
Pore size (mm)	0.821 ± 0.041	0.580 ± 0.039	0.285 ± 0.026	0.840 ± 0.057	0.537 ± 0.033	0.258 ± 0.037
Strut size (mm)	0.914 ± 0.028	0.594 ± 0.033	0.413 ± 0.017	0.898 ± 0.045	0.622 ± 0.050	0.448 ± 0.039
Porosity (%)	52.1 ± 0.95	45.4 ± 3.21	32.1 ± 3.50	52.9 ± 2.17	43.8 ± 2.21	30.5 ± 3.30
Surface/Volume (mm^2/mm^3)	4.57 ± 0.22	4.54 ± 0.15	5.40 ± 0.17	4.65 ± 0.25	4.88 ± 0.31	5.43 ± 0.59

Table 2

Tissue Mineral Density, Bone Volume and Modulus of scaffold and tissue constructs at 4 and 8 weeks

		PLLA			50:50PLGA		
		Large	**Medium**	**Small**	**Large**	**Medium**	**Small**
TMD (mg/cc)	4 wk	462.6 ± 12.4 (N=4)	463.4 ± 12.5 (N=5)	482.4 ± 12.1 (N=5)	482.8 ± 14.0 (N=8)	477.5 ± 21.7 (N=7)	476.2 ± 16.4 (N=5)
	8 wk	524.8 ± 21.4 (N=3)	546.0 ± 14.7 (N=5)	536.5 ± 24.4 (N=5)	534.5 ± 31.4 (N=5)	519.9 ± 22.5 (N=5)	528.7 ± 29.2 (N=5)
Bone Volume (mm^3)	4 wk	13.96 ± 5.14 (N=4)	17.37 ± 6.53 (N=5)	18.66 ± 13.87 (N=5)	8.58 ± 2.08 (N=8)	11.61 ± 3.28 (N=7)	10.39 ± 2.27 (N=5)
	8 wk	9.83 ± 0.89 (N=3)	11.25 ± 3.85 (N=5)	14.71 ± 4.28 (N=5)	13.88 ± 4.76 (N=5)	15.55 ± 4.38 (N=5)	21.77 ± 11.96 (N=5)
Modulus (MPa)	0 wk	100.4 ± 56.4 (N=7)	98.9 ± 30.6 (N=7)	196.4 ± 76.7 (N=7)	197.8 ± 53.7 (N=6)	239.0 ± 102.6 (N=6)	125.1 ± 63.2 (N=5)
	4 wk	13.0 ± 4.2 (N=4)	29.4 ± 14.2 (N=4)	90.5 ± 41.7 (N=7)	0.78 ± 0.35 (N=5)	1.30 ± 0.73 (N=6)	0.80 ± 0.40 (N=4)
	8 wk	32.2 ± 31.9 (N=3)	53.7 ± 28.1 (N=5)	83.4 ± 27.3 (N=5)	5.43 ± 5.97 (N=5)	4.15 ± 1.79 (N=4)	6.62 ± 3.52 (N=4)